Regenspurg, S., Driba, D. L., Zorn, C. (2016): Formation and significance of laurionite in geothermal brine. - *Environmental Earth Sciences*, *75*, 865

DOI: http://doi.org/10.1007/s12665-016-5668-4

Title page:

Authors: Simona Regenspurg[1*], Dejene Legesse Driba[1], Carolin Zorn[1]

Title: Formation and significance of laurionite in geothermal brine

Affiliations:

[1] Helmholtz Centre Potsdam
GFZ German Research Centre for Geosciences
Section 4.1 Reservoir Technologies
International Centre for Geothermal Research (ICGR)
Telegrafenberg, D-14473 Potsdam, Germany

* corresponding author: email: regens@gfz-potsdam.de; phone:+49 (0)331 288 1437

Abstract

The metal lead (Pb) is an environmentally significant, frequently occurring element in geothermal brines. It was found to precipitate from saline fluids predominantly as laurionite (PbOHCl) forming one of the most dominant scaling minerals identified at the geothermal site Groß Schönebeck (Germany). In this study, its formation conditions and relevance for the environment are investigated and discussed. To simulate laurionite precipitation, various amounts of base (NaOH) were added to solutions containing 3 M NaCl, 1 M $CaCl_2$, and 10 mM $Pb(NO_3)_2$ at 25 °C, 80 °C, and 133 °C. The formed precipitates were analyzed by X-ray diffraction and scanning electron microscopy. In nearly all experiments laurionite had formed as the predominant/ only mineral. Experimental results showed the same trends for equilibrium calculations performed with the code PhreeqC and the database "geodat". The results indicate that the formation of laurionite from geothermal, Pb-bearing saline brine is very probable, with the pH value as the main controlling parameter for its formation. It can be assumed that laurionite plays an important role in these systems not only by removing Pb from the brine but also by buffering the pH value in the fluid. Since scales removed from geothermal wells often contain significant amounts of the radioactive ^{210}Pb isotope, it can be assumed that the mineral laurionite acts as scavenger for this isotope and is therefore of environmental relevance. Adequate disposal and handling of the formed scales need to be considered.

Keywords

Laurionite, scaling, lead, geothermal, chloride, pH control

1 Introduction

Saline, geothermal fluids from deep sedimentary basins or from crystalline rocks are often enriched in toxic and/or radioactive metals such as copper (Cu), arsenic (As), lead (Pb), or radium (Ra) (Kharaka & Hanor 2004; Regenspurg et al., 2010; 2014). These elements accumulate in the formation water due to their long term interactions between water and the host rock as well as due to the formation of aqueous complexes between the metals and ligands such as chloride complexes that prevent the metals from precipitation (Frape et al. 2004, Kharaka & Hanor 2004). Lead often occurs in very high concentrations in geothermal fluids for example with up to 95 to 96 ppm (as Pb^{2+}) in brines from the Salton Sea and Soultz geothermal sites, respectively (McKibben et al. 1987; Scheiber et al. 2013). It is of special relevance in these systems not only because it is very toxic, but also because deep formation fluids often carry elevated amounts of the natural radioactive isotope ^{210}Pb (an intermediate decay product of the uranium-238 series) with a half-life of 22.2 years (Takahashi et al. 1987). In presence of sulphate, sulphide, carbonate, or oxide, Pb^{2+} forms some hardly soluble salts (e.g. $PbSO_4$, PbS, $PbCO_3$, PbO) thereby removing the Pb from the aqueous phase. When producing geothermal brine for heat or electricity production the physicochemical conditions of the brine often change resulting in a potential oversaturation of those salts. Mineral precipitations ("scaling") generally represent a problem for geothermal power plant operation because they are clogging pipes thereby reducing the fluid flow through the system or they are coating the heat exchanger and thus reducing the efficiency of the geothermal plant. If these precipitates form within the pores of a reservoir, it might even results in reservoir damage and in complete failure of the system. In addition, some of these solid residues collected from filters and pipes are often enriched with natural occurring radioactive isotopes such ^{210}Pb, ^{226}Ra, ^{228}Ra, ^{232}Th, and ^{238}U and have to be deposed adequately (Degering & Köhler, 2011).

The Pb mineral laurionite (PbOHCl) has recently been found to occur at some geothermal sites (e.g. Groß Buchholz and Groß Schönebeck) located in the North German Basin (Hesshaus et al. 2013; Regenspurg et al. 2015). At the Groß Schönebeck *in situ* geothermal research platform fluid production had to be terminated in 2013 due to decreasing production rates that possibly were linked to the simultaneous formation of massive scaling that accumulated in the production well, clogging it for nearly 200 m (Blöcher et al., 2015). Laurionite was detected as one of the four most dominant minerals (together with native copper, magnetite,

and barite) in the material that filled the well (Regenspurg et al. 2015). Laurionite can thus be considered as significant in those geothermal systems, although it is unclear at which chemo-physical conditions it actually forms.

The white or colorless orthorhombic hydroxy halogenide laurionite (Pb(OH)Cl) with clear cleavability at {101}, typically forms tabular, prismatic, or acicular crystals (Venetopoulos & Rentzeperis 1975). It is dimorph with the monoclinic paralaurionite that also crystallizes as prismatic and transparent shapes (Merlino et al. 1993). Both occur rarely in nature (Merlino et al. 1993) but can be found as formation product from Pb-bearing industrial waste or as secondary mineral in the oxidation zone of Pb-containing ore deposits (Russell, 1928; Palaehe, 1934). The very first description of laurionite was from several antique mining slag deposits in the area of Laurion (Attica, Greece; Köchlin 1887). These slag residues have been dumped into the sea about 2000 years ago, allowing the enclosed Pb to react with the chloride of sea water (Angel & Scharizer 1932). Laurionite, however also frequently forms as part of solid waste in lead smelters (Ioannidis et al. 2006). Artificially, laurionite has been produced by reaction of lead and sodium chloride and was used as make up already by the ancient Egypt (Walter et al., 1999; Hess, 1999) or as white pigment for medieval paintings (Hoyer 2010).

Edward et al. (1992) investigated in detail the mineral formation of the PbO-H_2O-HCl system at 292.2 K. At these conditions a range of lead minerals can form depending on the pH value and chloride content of the solution: cottunite ($PbCl_2$), penfieldite (Pb_2Cl_3OH), fiedlerite ($Pb_3Cl_4(OH)_2$), laurionite (PbOHCl), paralaurionite (PbOHCl), mendipite ($Pb_3O_2Cl_2$), blixite ($Pb_2Cl(OH)_3$, and litharge (PbO) have been observed in carbonate-free systems. As shown in the stability diagram with increasing pH and increasing salinity, the laurionite becomes more stable (Fig. 1, Edward et al., 1992). However, chloride activities used for these calculations (e.g. Fig. 1) were still clearly below concentrations of many geothermal brines especially of those hosted in sedimentary basins (Kharaka & Hanor 2004), such as measured at the geothermal site of Groß Schönebeck (about 5 M chloride; Regenspurg et al. 2010).

Consequently, most databases used for geochemical equilibrium calculations, for example those included in the code PhreeqC (Parkhurst & Apello 2013), do not contain laurionite and its equilibrium constants as mineral species. Solely the MINTEQA2 version 4 and WATEQ4F database (Peterson et al. 1987; Allison et al. 1990;U EPA, 1998, Ball & Nordstrom, 2001) consider laurionite and gives a solubility constant of log K = 0.623 for $PbOHCl + H^+ = Pb^{2+} + Cl^- + H_2O$. The llnl database considers paralaurionite with a log K = 0.2035 (Wolery 1992).

However, in both the MINTEQA2 and in the WATEQ4F database, enthalpies are not included for laurionite and thus they should not be used for calculations at higher temperatures. Moreover, the activity coefficient calculations included in these databases either apply the extended (Wateq) Debye-Hückel attempt which is valid up to 0.7 mol/Kg or the Davies equation which goes up to 0.5 mol/kg. For solutions of higher salinities (like in many geothermal brines) the Pitzer equations should be used. The Geodat thermodynamic database has been recently developed especially for applications at geothermal conditions (Moog & Cannepin 2014). It can be implemented in other geochemical codes such as PhreeqC and calculates metal speciation explicitly for highly saline solutions. The database includes various lead chloride species as a function of temperature and ionic strength based on the stability constants from Luo & Millero (2007). It allows determining lead chloride speciation with Pitzer activity coefficients for ionic strengths from 0 to 6 M and for up to 300 °C although no T-dependent solubility data for laurionite are available.

Due to limited data availability and restricted potential to perform geochemical equilibrium modeling, the aim of this experimental study was to investigate if and at which geothermal-similar conditions laurionite can form and if the application of equilibrium modeling by using the Geodat database shows similar trends as observed by the experimental data. The prediction of potential laurionite formation in a geothermal system is of high relevance for geothermal well operation in order to develop methods of avoiding Pb scaling and thus reducing the enrichment of radioactive ^{210}Pb in the above ground installation or in the solid waste (e.g. filter residues).

2 Materials and Methods

A stock solution containing 3 M sodium (Na), 1 M calcium (Ca), 5 M chloride (Cl) and 10 mM $Pb(NO_3)_2$ was prepared from analytical grade salts. This solution was visually clear with a measured pH of 6.2. The pH measurements were performed with a WTE glass electrode that allow measurements up to 100 °C. It needs to be considered that when the salinity of the sample solution is larger than the ionic strength of the buffering electrolyte (usually 3 M KCl) of the probe, measurements with ion-selective electrodes such as most pH probes are affected by the salt content resulting in a shift of the measured pH value (Altmaier et al. 2003). This shift can be determined for individual electrodes according to Altmaier et al. (2003) and is about one pH-unit for the pH-probe applied in this study in a 5 M chloride solution (Feldbusch et al. 2013). To obtain thus the actual (real) pH value (corresponding to the activity

of hydronium ions (=-log {H}), the pH-shift (determined in dependence of temperature and salinity) has to be added to the measured value. In this study, however, just the measured (uncorrected values) are usually presented for better comparison with field data.

Different neutral to basic pH values were adjusted to the saline Pb containing solutions by titration of 50 mL stock solutions with 1 M NaOH. The obtained suspensions were kept either in glass bottles at ambient conditions or in PTFE reactors at 80 °C in the oven (Deon et al. 2013), or at 133 °C and 10 bar in autoclaves (Banks et al. 2014).

The pH was measured in the solutions kept at 25 °C and 80 °C after 1, 2, 4, 5, 6, and 24 hours. Afterwards, the formed precipitates were separated from the solutions by filtration (paper filter). The filter residues were washed with deionized water and dried at 105 °C in the oven. The mass of the residues was determined by weighing (accuracy of 0.1 mg) and the formed solid phases were analyzed visually with an optical microscope. For X-ray diffraction (XRD) preparation, samples were first ground to a homogenous powder with an agate mortar. The powder was afterwards analyzed with a diffractometer equipped with a Cu Kα1 radiation source, a primary monochromator, and a 7°-wide position 9 sensitive detector. The obtained diffractograms were qualitatively evaluated by the XRD software EVA (diffrac.suite; Bruker). For scanning electron microscopy (SEM) samples were gold-vaporized and a beam current acceleration of 20 kV, and a maximum aperture of 120 µm were adjusted. The material composition was semi-quantitatively characterized by energy dispersive X-ray (EDX), using the same accelerating voltage on selected image spots. In addition, solid samples were analyzed after carbon vaporization with the electron micro probe JXA 8200.

Geochemical equilibrium modeling was performed with PhreeqC v3 (Parkhurst and Apello 2013) using the Geodat database (Moog and Cannepin 2014). The latter includes the Pb chloride complexes and equilibrium constants as summarized in Table 1. Lead speciation calculations were performed for solutions with 5 M and 0.5 M chloride solution and containing 1 mM Pb.

3 Results

In all prepared experimental solutions, the addition of just a small amount from the 1 M NaOH into the stock solution (10 mM Pb +1 M $CaCl_2$+3 M NaCl) resulted immediately in the formation of a cloudy, white precipitate that dissolved again during stirring until a total of at least 4 mM NaOH were added.

During the titration the measured pH value increased significantly between 4 and 12 mM added NaOH from 6.2 to around 10.5 at room temperature (Fig. 2). Within the experimental period of 24 h, the curve flattened slightly but the final pH value remained relatively constant (10.4-10.8; open symbols in Fig. 2). Solutions kept at 80 °C show a similar titration curve but the final pH is clearly lower and more variable as compared to the curves of samples kept at room temperature (8.8-9.5). Since the pH was still slightly decreasing, the final equilibrium was apparently not obtained after 24 h in all experiments.

The amount of solid phases formed at constant Pb concentration, depends on both, the added amount of NaOH and the temperature (Fig. 3). In general the produced mass increased with increasing OH^- addition but for experiments at 25°C and 133 °C less mass precipitated when 8 mM added NaOH. With increasing temperature the precipitated mass also increased but decreased at T > 80°C again. Most mass formed at around 80 °C and with 9 to 10 mM OH^- added (Fig. 3). The highest amount (2.25 g/L) was measured in the sample kept at 80 °C with 17 mM OH^- added.

Geochemical equilibrium speciation calculations of Pb-chloro complexes indicated that at the highest ionic strength (5 M), negatively charged Pb-chloride ($PbCl_3^-$) complexes dominated in the solutions, whereas at 0.5 M NaCl, Pb occurs predominantly as positively charged $PbCl^+$ or free Pb^{2+} ion (Fig. 4). With increasing temperature (e.g. 150 °C, dashed lines in Fig. 4) the amount of $PbCl_3^-$ and $PbCl^+$ also increased with simultaneous decrease of $PbCl_4^{2-}$ and Pb^{2+}, respectively.

Increasing Cl^- and decreasing temperature increase the saturation index (SI) of laurionite which becomes oversaturated in a 5 M NaCl solution at pH > 6.4 (for 25 °C) and > 6.6 (at 150 °C; Fig. 5). The calculated amount of Pb precipitated as laurionite was relatively small for solutions containing 0.5 M NaCl (< 1.2 % and 1 % for pH 9 and 7, respectively) and higher for a 5 M NaCl solution, when 9 % of the total Pb concentration would precipitate as laurionite at pH 7 and 12.2 % at pH 9. With increasing temperature the amount of precipitated Pb decreased. Below pH 6.4 laurionite was never saturated at investigated conditions.

X-ray diffraction gave clear evidence, that laurionite had formed in almost all experiments, because obtained diffractograms fit well with laurionite from the library database of the evaluation software (Fig. 6, top). As additional phase portlandidte ($Ca(OH)_2$) was observed in samples with 17 mM NaOH at 25 and 80 °C. The only exception with no identified laurionite peaks is the precipitate that formed in the most alkaline solution (17 mM NaOH) kept at

highest temperature of 133 °C. Here, the XRD pattern fits to 100 % with the mineral mendipite ($Pb_3O_2Cl_2$; Fig. 6, bottom). This sample had also a different optical appearance in as much it was of yellowish color, whereas all other precipitates were white.

Investigations with optical and scanning electron microscope and electron microprobe showed different habitus of the precipitates in dependence of their formation conditions. Already with the optical microscope long- needle-like crystals are visible in samples formed at highest temperature (133°C). By analysis with the SEM, the crystals formed at room temperature showed a flat and tabular appearance ("tree bark"; Fig. 7) and with increasing temperature, when 11 mM NaOH were added, they developed short, oval shapes (at 80 °C; Fig. 7) with some prismatic portlandite ($Ca(OH)_2$) in between as identified by elemental analysis with EDX. No portlandite was found at 133 °C, instead the length of the laurionite crystals increased forming thin needles of up to 1 mm length. Mendipite, which precipitated, as evidenced by XRD (Fig. 6), both, at highest OH^- concentration and highest temperature also forms fibrous aggregates and can, therefore, not visually be differentiated from laurionite.

4 Discussion

4.1 Comparison of experimental and modeling data

Results from the experimental study as well as from geochemical equilibrium calculations showed that laurionite formation depends mainly on the chloride concentration and the pH value of a solution, whereas temperature plays a minor role. In a geothermal system with rather constant Pb and Cl concentrations, the pH value alone controls laurionite formation. It was demonstrated that at a given Pb concentration at experimental conditions, laurionite was oversaturated already when a minimum concentration of NaOH was added to the solution (4 mM) that resulted in a measured pH value of 6.48 (at 80 °C) and 6.55 (at 25 °C; Fig. 2), whereas at a pH of 6.2 no precipitation was observed. Geochemical calculations confirmed this observation (laurionite saturation starting at pH > 6.7 in 1 mM Pb^{2+}) of increased precipitation with increasing amount of added hydroxide demonstrating further that positively charged lead (Pb^{2+}) requires high chloride concentrations to form negatively charged, stable Pb-chloro complexes. In the presence of excess hydroxide in solution, these OH^- ions are attracted to the partly positively charged lead-chloro complexes. Thereby the solutions oversaturate and eventually precipitate as laurionite. Evidently, modeling and experimental results show the same trends, but cannot be directly compared because (i) experiments were not fully in

equilibrium after 24 h (Fig. 2); (i) for modeling, a concentration of 1 mM Pb was used (similar to the natural Pb concentration in geothermal brine), whereas in the experiments 10 mM Pb were added to the stock solutions; (iii) the database used for modeling does not contain solubility data for increased temperatures for laurionite. Assuming that the complete amount of formed precipitates in experiments at pH < 10 is pure laurionite, than up to 85.7 % of all Pb has precipitated during the experiments from a 10 mM Pb solution (corresponding to 2.25 g/L), whereas in the modeling calculations, a maximum of 12.2 % of Pb would form laurionite from a 1 mM Pb solution.

Laurionite was the predominant mineral forming in all experiments up to pH values <10 and below 133 °C when mendipite became the most stable mineral. Mendipite, however, was not part of the databases used for geochemical modeling and therefore it was not possible to calculate saturation indices for mendipite.

4.2 Laurionite formation in the geothermal production well of Groß Schönebeck

In deep sedimentary basins temperatures and pH values of geothermal brines vary depending on depth and type of the geological host rocks. In the sandstone formation of the Groß Schönebeck geothermal reservoir, the pH values of the formation fluid are usually around neutral (5.5-7) and the maximum temperature at depth of the reservoir is 150 °C in about 4100 m (Huenges et al., 2006). Assuming that at reservoir conditions the Pb concentration of the Groß Schönebeck brine (about 1 mM; Regenspurg et al. 2010) is in equilibrium, a slight pH increase along the water column is most likely responsible for oversaturation and the observed laurionite precipitation. The pH values normally determined in Groß Schönebeck fluids, measured in samples collected from the well bottom are between 5.5 and 6.2 (Regenspurg et al. 2010; 2015) whereas in samples collected above ground the pH ranges between 6.5 and 7 (Feldbusch et al., 2013). Thus, saturation of laurionite that has been determined to occur above pH 6.4 (Fig.5) can be expected. The reason for the pH variation within the Groß Schönebeck geothermal well is not evident so far. Since laurionite was mainly found in the wellbore fill, formed at the bottom of the production well and only in small quantities in filter residues (the thermal was filtered above ground before reinjection into the reservoir), its formation seems to be connected to processes within the wellbore. Three possible mechanisms are considered for the pH shift: (i), laurionite uses hydroxide from H_2O for its formation thereby an access of acid is released that is immediately consumed by other

processes in the wellbore such as corrosion of the casing or calcite dissolution. Evidence of both, casing corrosion and the occurrence of small amounts of calcite have been observed at the Groß Schönebeck geothermal site (Regenspurg et al. 2015). Another explanation for a pH shift (ii) could be that degassing of CO_2, dissolved in the brine slightly shifts the pH to higher values. Although the CO_2 content of the Groß Schönebeck fluid is relatively small (< 5 vol-%; Regenspurg et al. 2010) and degassing of most of the CO_2 is actually prevented by adjusting the pressure to about 10 bar in the above ground installation (Frick et al. 2011), the release of some CO_2 was calculated to begin at a depth of 2986 m within the Groß Schönebeck production well (Francke, 2014). According to this wellbore model, the calculated pH increase from the well bottom to above ground would explain a pH increase from 6.4 to 6.95 (Driba, 2015), which would be sufficient for laurionite precipitation. A third explanation (iii) is based on an observation of the wellbore fill: When samples of this material were collected by bailers in 2012 from the bottom of the well, the pH value was measured in the pore water of this mud-like material. While in most of these mud samples the pH values were neutral, in one sample (GrSk 119; collected August 2012; Regenspurg et al. 2015), a pH of 11.5 was measured in the pore water of the collected mud (unpublished data). Since this was a much localized observation (one sample, collected from one specific depth: 4112m), we explain this measurement with partly dissolving cementation that is installed behind the casing. Cement, in general, consists predominantly out of hydroxides (e.g. portlandite), that are highly alkaline (pH > 11). Therefore dissolution of cement could release hydroxide ions thus being responsible for the strongly increased pH value. This particular bailer sample was collected at a depth were the liner is perforated, which implies that a contact reaction between the wellbore fluid and the cementation is possible. Close to the area where those hydroxides would be swept into the well, Pb could immediately react with them and precipitate as hydroxide (e.g. laurionite). If that is indeed the case, the laurionite precipitation in Groß Schönebeck is caused by material failure due to instability of the cementation. This theory is supported by the observed shapes of this “field” laurionite which shows long, thin needles in the SEM picture (Regenspurg et al. 2015; Fig. 8) indicating a high formation temperature > 133 °C that is only achieved at depth in the wellbore (about 150 °C at reservoir conditions), whereas if CO_2 release would be the driving force for pH increase, the laurionite would have formed at cooler temperatures closer so the earth´s surface and would thus show different shapes (Fig. 7). Another indication for the cementation-dissolution theory is by comparing the amount of dissolved Pb, measured in

the water column or in above ground installations, respectively. Despite higher pH values during producing conditions measured above ground, the Pb concentration in the fluid ranged between 140 and 160 ppm. In contrast, when deep fluid samples were collected in the well bottom during shut-in times, the Pb concentration decreased (despite lower pH values) to below 5 ppm as measured in samples from 2012 and 2013. This indicates that at wellbore conditions also the kinetics might control laurionite formation showing that most laurionite formed at stagnant conditions.

4.3 Environmental significance of laurionite formation

Laurionite is an environmentally significant mineral, because it removes toxic Pb including the radioactive ^{210}Pb isotope from the brine, and enriches them in the formed scales. At the Groß Schönebeck site, elevated ^{210}Pb activities of up to 102 Bq/l were measured in the geothermal brine (Regenspurg et al., 2014) and solid phases collected at the site (filter residues or material from the wellbore fill) even contained up to 24 kBq/kg of ^{210}Pb (Regenspurg et al. 2014). Increased amounts of radioactive lead in scaling from above ground geothermal installations are also known from other geothermal sites such as Soultz-sous-Forets or Neustadt Glewe (Scheiber et al., 2012; 2013; Degering et al., 2011). At the Soultz-sous-Forets site Pb scales represent a specific problem, after other scale formation (such as barite) was successfully prevented by application of scale inhibitors leaving the remaining scale (mainly galena, PbS) to be enriched with the radioactive Pb. These “purer” Pb-scales are consequently less diluted with other scaling minerals and therefore of higher radioactivity. Therefore the disposal of these enriched scales represents a severe challenge for power plant operators that is to date not yet solved.

Apart of its role as toxic and radioactive component, experiments performed in this study have shown that laurionite immediately forms upon pH-increase in simulated geothermal brine. Thereby laurionite removes hydroxide from solution and adjusts the pH to around 6.5. Thus laurionite is assumed to play an important role as pH buffer in geothermal systems where sufficiently high Pb and chloride concentrations can be expected.

5 Conclusions

The present study demonstrated the likeliness and relevance of laurionite formation in geothermal brines that contain elevated Pb concentrations. At given experimental conditions (10 mM Pb, 3 M NaCl, 1.5 M $CaCl_2$, T < 133°C, neutral to basic pH) laurionite starts immediately

to precipitate and shows the same trend as results calculated with the equilibrium program PhreeqC and the geodat database for the same conditions. Experimental results also fit well to field observations from the Groß Schönebeck geothermal site, where large amounts of laurionite have been identified in the scales removed from the well. Due to the apparently frequent occurrence of laurionite in these systems, there is high need for accurate prediction of its formation conditions in order to estimate the scaling potential and eventually to prevent it. For this reason, databases should further be developed and solubility data need to be validated for higher temperatures. Stability diagrams as shown in Fig. 1 should be extended to both, higher chloride concentrations and higher temperatures.

To prevent laurionite formation in a geothermal well, basically two methods can be considered: either the pH value would be slightly decreased by acidifying to around pH six or inhibitors could be added to prevent Pb mineral precipitation. Adequate inhibitors, however, have so far not been applied for geothermal brines and need first to be tested for their effectivity and stability at given geothermal conditions.

For the Groß Schönebeck geothermal site a localized pH increase was observed that was possibly induced by damaged casing material and cementation dissolution. Therefore, it needs to be validated if the wellbore completion of the GrSk production well is still intact. A multi caliper measurement could indicate if a larger damage to the casing and cementation occurred at the depth (4205 m), where the bailor sample with the very high pH value (11.5) of the mud pore water was collected.

Finally, the present study has to be considered as preliminary, because larger ranges of physico-chemical conditions should be investigated as well. Additional lab experiments should be performed with a similar set-up as demonstrated in this study but that also includes more pH measurements (over a broader range and titration with more increments) and a greater temperature and salinity range (e.g. up to 200 °C and 1 to 10 M chloride). Of especial importance would be that the experiments last over a longer time period to ensure equilibrium and to measure additionally aqueous Pb in solution for mass balance.

Acknowledgments

We kindly acknowledge Ilona Schäpan and Rudolf Naumann for assisting in measuring with the scanning electron microscope and the X-ray diffraction. Thanks also to Ralf Milke (FU Berlin) for measuring at the electron microprobe. Many thanks go to Marco di Lucia (GFZ) for support in geochemical modeling.

Funding of this study was provided within the project “GeoDat” (Development of thermodynamic data for equilibrium modeling of processes in deep geothermal formations) by the German Federal Ministry for the Environment, Nature Conservation and Nuclear Safety (BMU) and later by the Ministry for Economic Affairs and Energy (BMWi).

References

Allison JD, Brown DS, and Novo-Gradac KJ (1991) MINTEQA2/PRODEFA2—A geochemical assessment model for environmental systems—Version 30 user’s manual: Athens, Georgia, Environmental Research Laboratory, Office of Research and Development, US Environmental Protection Agency, 106 p

Altmaier M, Metz V, Neck V, Müller R, Fanghänel TH (2003) Solid-liquid equilibria of $Mg(OH)_2$(cr) and $Mg_2(OH)_3Cl\_4H_2O$(cr) in the system Mg-Na-H-OH-Cl-H_2O at 25 °C. Geochim Cosmochim Acta 67(19), 3595–3601

Angel F, Scharizer R (1932) Grundriss der Mineralparagenese. Springer, Wien, 293 p

Ball W, Nordstrom D K (2001) User´s manual for WATEQ4F, with revised thermodynamic data base and test cases for calculating speciation of major, trace, and redox elements in natural waters. US Geological survey, open file report 91-183.

Banks J, Regenspurg S, Milsch H (2013) An experimental method for determining scaling risks in basin-hosted Enhanced Geothermal Systems: an example from the Na-Ca-Sr-Ba-Cl-SO4-H2O system. Applied Geochemistry 47, 74-84

Degering D, Köhler M, Hielscher M (2011) Vorkommen und Verhalten natürlicher Radionuklide im Aquifer, im Fluid und in den Ablagerungen der Geothemieanlage Neustdt-Glewe. Z. geol. Wiss., Berlin 39 (3/4), 275-290

Deon F, Regenspurg S, Zimmermann G (2013) Geochemical interactions of Al_2O_3-based proppants with highly saline geothermal brines at simulated in situ temperature conditions. Geothermics 47, 43-61.

Driba (2015) Experimental characterization and simulation of lead surface reactions for application at geothermal conditions. PhD Thesis, Technical University of Berlin

Edwards R, Gillard RD, Williams PA, Pollard AM (1992) Studies of secondary mineral formation in the PbO-H2O-HCl system. University of Wales College, Cardiff, United Kingdom; p 53-65

Feldbusch E, Regenspurg S, Banks J, Milsch H, Saadat A (2013) Alteration of fluid properties during the initial operation of a geothermal plant: results from in situ measurements in Groß Schönebeck. Environmental Earth Sciences 70 (8), 3447-3458

Francke H (2014) Thermo-hydraulic model of the two-phase flow in the brine circuit of a geothermal power plant. PhD thesis, Technical University of Berlin (Germany)

Frape SK, Blyth A, Blomqvist R, McNutt RH, Gascoyne M (2004) Deep fluids in the continents: II. Crystalline rocks. In: Surface and Ground Water, Weathering, and Soils (eds. Drever JI, Holland HD, Turekian KK), Treatise on Geochemistry, 541–580. Elsevier, Amsterdam

Frick S, Regenspurg S, Kranz S, Milsch H, Saadat A, Francke H, Brandt W, Huenges E (2011) Geochemical and process engineering challenges for geothermal power generation. Chemie Ingenieur Technik 83 (12), 2091-2104

Hess W (1999) Hightech-Kosmetik der Pharaonen erforscht. www.wissenschaftde/ Leinfelden-Echterdingen

Hesshaus A, Houben G, Kringel R (2013) Halite clogging in a deep geothermal well – Geochemical and isotopic characterization of salt origin. Physics and Chemistry of the Earth 74, 127-139

Hoyer S (2010) Die Wandmalereien der Dominikaner in Bamberg – Kunsttechnologische Analyse des Malereibestandes und beispielhafte Vermittlung komplexer Zeitschichten. Bamberg, Univ, Diss, 2010

Huenges E, Trautwein U, Legarth B, Zimmermann G (2006), Fluid pressure variation in a sedimentary geothermal reservoir in the North German Basin: Case study Groß Scho¨nebeck, Pure Appli. Geophys. 163, 2141–2152

Ioannidis ThA, Zouboulis AI, Matis KA (2006) Effective treatment and recovery of laurionite-type lead from toxic industrial solid wastes. Separation and Purification Technology 48 (2006) 50–61

Kharaka YK, Hanor JS (2004) Deep fluids in the continents: I: Sedimentary rocks, in: Drever, JL, Holland, HF, Turekian, KK (eds), Treatise on Geochemistry, vol 5, Surface and groundwater, weathering, and soils, 499 – 540

Köchlin R (1887) Ueber Phosgenit und ein muthmasslich neues Mineral vom Laurion. Annalen des KK Naturhistorischen Hofmuseums, 2, 185-190

Luo Y, Millero FJ (2007) Stability constants for the formation of lead chloride complexes as a function of temperature and ionic strength Geochim Cosmochim Acta 71,326–334

McKibben MA,Williams TE, Ellders WA, Eldridge CS (1987) Saline brines and metallogenesis in a modern sediment-filled rift: the Salton Sea geothermal system, California, U.S.A. Applied Geochemistry 2, 563-578

Moog HC, Cannepin R (2014) Entwicklung von thermodynamischen Daten für die Belange der thermodynamischen Gleichgewichtsmodellierung von Prozessen in tiefen, geothermalen Schichten Teilprojekt A (GRS): Bestimmung von Ionenwechselwirkungs-koeffizienten und Aufstellung eines Reservoirmodells 165p GRS - A - 3749 ISBN-Nr 978-3-944161-17-4. www.grs.de/sites/default/files/pdf/grs-337.pdf

Merlino S, Pasero M, Perchialli N (1993) Crystal structure of paralaurionite and its OD relationships with laurionite. Mineralogical Magazine 57, 323-328

Palaehe C (1934) The form relations of the leadoxychlorides, laurionite, paralaurionite, and fiedlerite. Mineral Mag, 23,573-86

Parkhurst DL (2013) User's guide to PHREEQC -A computer program for speciation, reaction-path, advective-transport, and inverse geochemical calculations: US Geological Survey Water-Resources Investigations Report 95-4227, 143 pSR

Peterson SR, Opitz BE, Graham MJ and Eary LE (1987) An Overview of the Geochemical Code MINTEQ: Applications to Performance Assessment for Low-Level Wastes. PNL-6112, March 1987

Peterson SR, Hostetler CJ, Deutsch WJ, Cowan CE (1987): MINTEQ User's Manual NUREG/CR-4808 (PNL-6106)

Regenspurg S, Wiersberg T, Brandt W, Huenges E, Saadat A Schmidt K, Zimmermann G (2010) Geochemical properties of saline geothermal fluids from the in-situ geothermal laboratory Groß Schönebeck (Germany). Chemie der Erde – Geochemistry 70 (3), 3-12

Regenspurg S, Dilling J, Mielcarek J, Korte F, Schkade U-K (2014) Naturally occurring radionuclides and their geochemical interactions at a geothermal site in the North German Basin. Environmental Earth Sciences 72 (10), 4131-4140

Regenspurg S, Feldbusch E, Byrne J, Deon F, Driba LD, Henninges J, Kappler A, Naumann R, Reinsch T, Schubert C (2015) Mineral precipitation during production of geothermal fluid from a Permian Rotliegend reservoir. Geothermics 54, 122-135

Russell A (1928) On laurionite and associated minerals from Cornwall. Mineral Mag 21,221-8

Scheiber J, Nitschke F, Seibt A, Genter A (2012) Geochemical and mineralogical monitoring of the geothermal power plant in Soultz-sous-Forets (France). In: Proceedings, 37th workshop on geothermal reservoir engineering, Stanford University, Stanford, 30 Jan–1 Feb 2012

Scheiber J, Seibt A, berner J, Genter A, Moeckes W (2013) Application of a Scaling Inhibitor System at the Geothermal Power Plant in Soultz-sous-Forêts: Laboratory and On-site Studies. European Geothermal Congress EGC, 2013

Takahashi K, Boyd RN, Mathews GJ, Yokoi K (1987) Bound-state beta decay of highly ionized atoms. Physical Review C 36 (4)

US Environmental Protection Agency (1998) MINTEQA2/PRODEFA2, A geochemical assessment model for environmental systems—User manual supplement for version 40: Athens, Georgia, National Exposure Research Laboratory, Ecosystems Research Division, 76 p Revised September 1999

Venetopoulos CC, Rentzeperis PJ (1975) The crystal structure of laurionite, Pb(OH)Cl. Zeitschrift für Kristallographie 141, 246-259

Walter P, Martinetto P, Tsoucaris G, Brniaux R, Lefebvre MA, Richard G, Talabot J, Dooryhee E (1999) Making make-up in Ancient Egypt. Scientific Correspondence Nature 397, 483-484 doi: 10.1038/17240

Wolery T (1992) Eq3/6, a software package for geochemical modeling of aqueous systems: Package overview and installation guide (version 70) ucrl-ma-110662 Technical Report, Lawrence Livermore National Laboratory, Livermore

Figure description

Fig. 1 Stability diagram for the PbO-HCl-H_20 system at 298.2 K and $l0^5$ Pa (Edwards et al., 1992).

Fig. 2 Titration of lead chloride solution (10 mM $Pb(NO_3)_2$ + 3 M NaCl + 1.5 M $CaCl_2$) solution with 1 M NaOH. The pH was measured at different time steps at 25 °C (open symbols) and 80 °C (full symbols). The red line gives the immediately measured pH values.

Fig. 3 Produced mass precipitated in dependence of added NaOH (left) or temperature (right).

Fig. 4 Predominance diagram of aqueous Pb species (Pb(II)-chloro complexes) as function of total Cl^- concentration, calculated for 25 °C (solid lines) and 150 °C (dashed lines) in a 10^{-3} M Pb solution by PHREEQC v.3 using the Geodat database (Cannepin & Moog, 2014). Numbers give the amount of Cl ions attached to the Pb complex.

Fig. 5 Calculated saturation index (SI) of laurionite from a 1 mM Pb solution as a function of pH, concentration of NaCl (0.5 and 5 M) and temperature as determined by PHREEQC v.3.0.6 (Parkhurst and Appelo, 2013).

Fig. 6 X-ray diffractograms of a synthesized sample produced at 25 °C and with 4 mM NaOH (top) and of a sample produced at 133 °C and with 17 mM NaOH (bottom), colored lines indicate the minerals according to the database.

Fig. 7 Scanning electron micrograph (SEM) electron microprobe pictures of synthesized minerals. All shapes correspond according to XRD predominantly to laurionite with the exception of the bottom right sample, which is a mendipite.

Fig. 8 Scanning electron micrograph of needle shaped, radial grown laurionite collected from the bottom of the Groß Schönebeck geothermal production (Regenspurg et al., 2015).

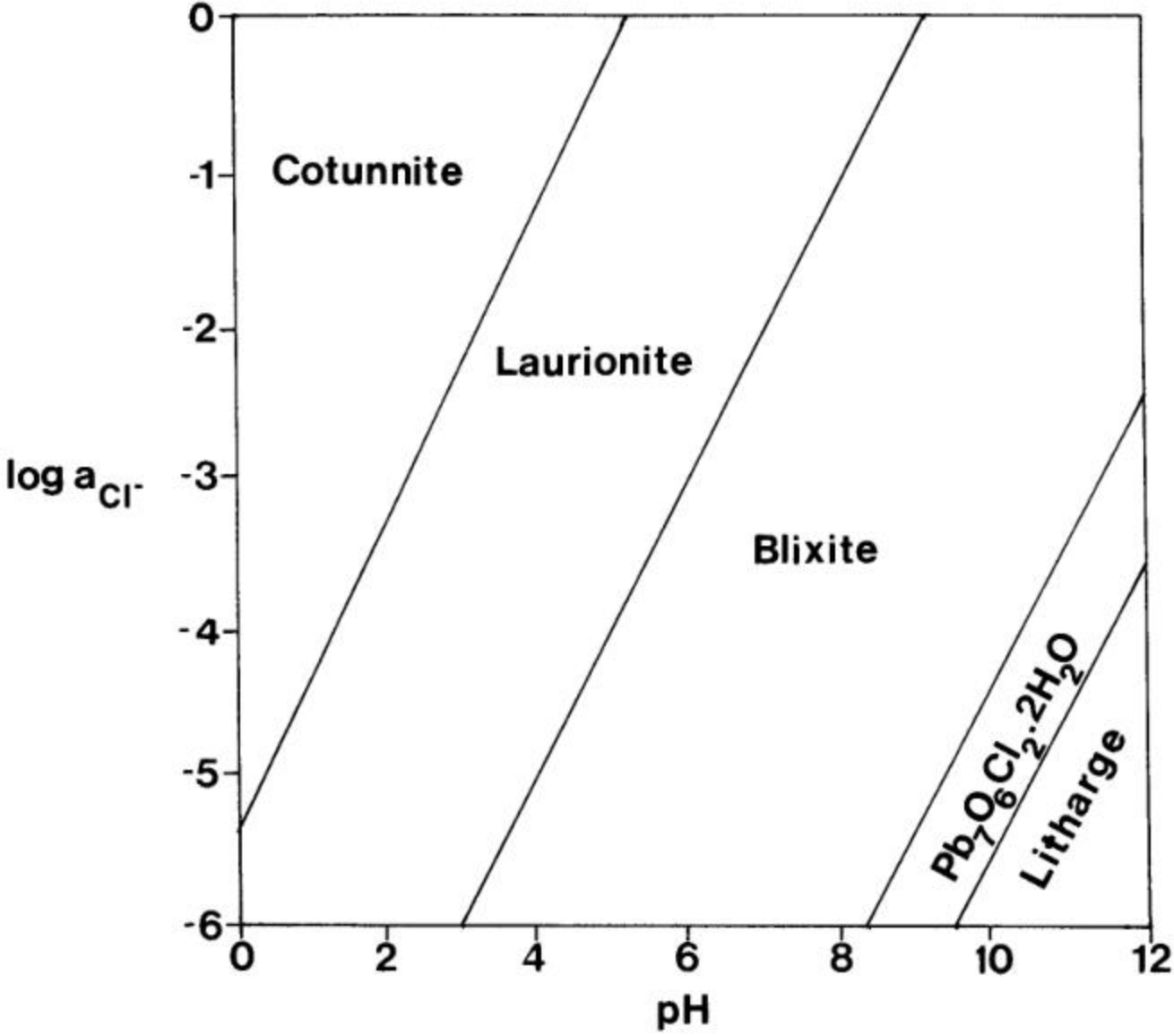
0
-1
-2
-3
-4
-5
-6
log a_{Cl^-}
Cotunnite
Laurionite
Blixite
$Pb_7O_6Cl_2 \cdot 2H_2O$
Litharge
0
2
4
6
8
10
12
pH

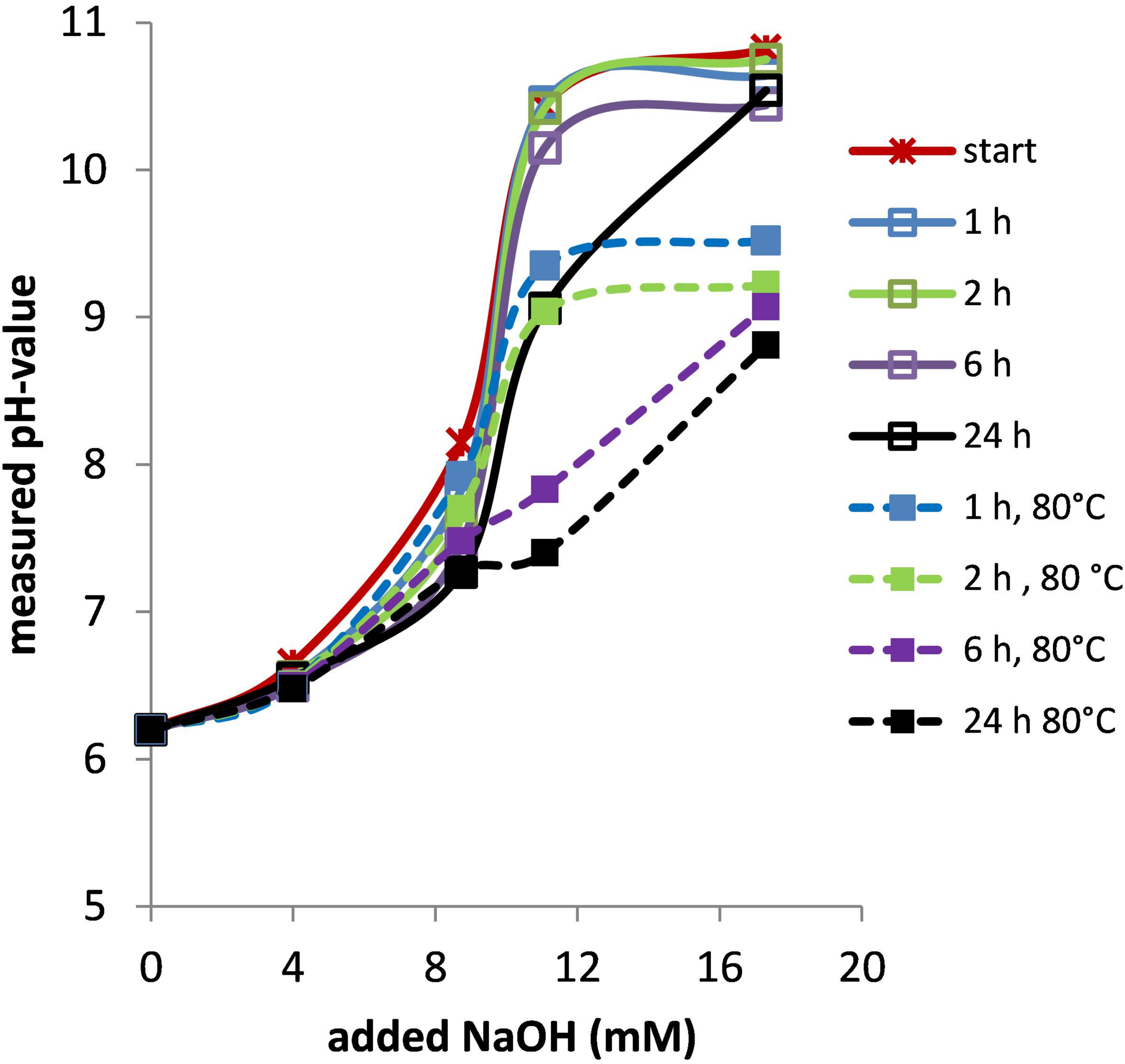
11
10
9
8
7
6
5
measured pH-value
0
4
8
12
16
20
added NaOH (mM)
start
1 h
2 h
6 h
24 h
1 h, 80°C
2 h , 80 °C
6 h, 80°C
24 h 80°C

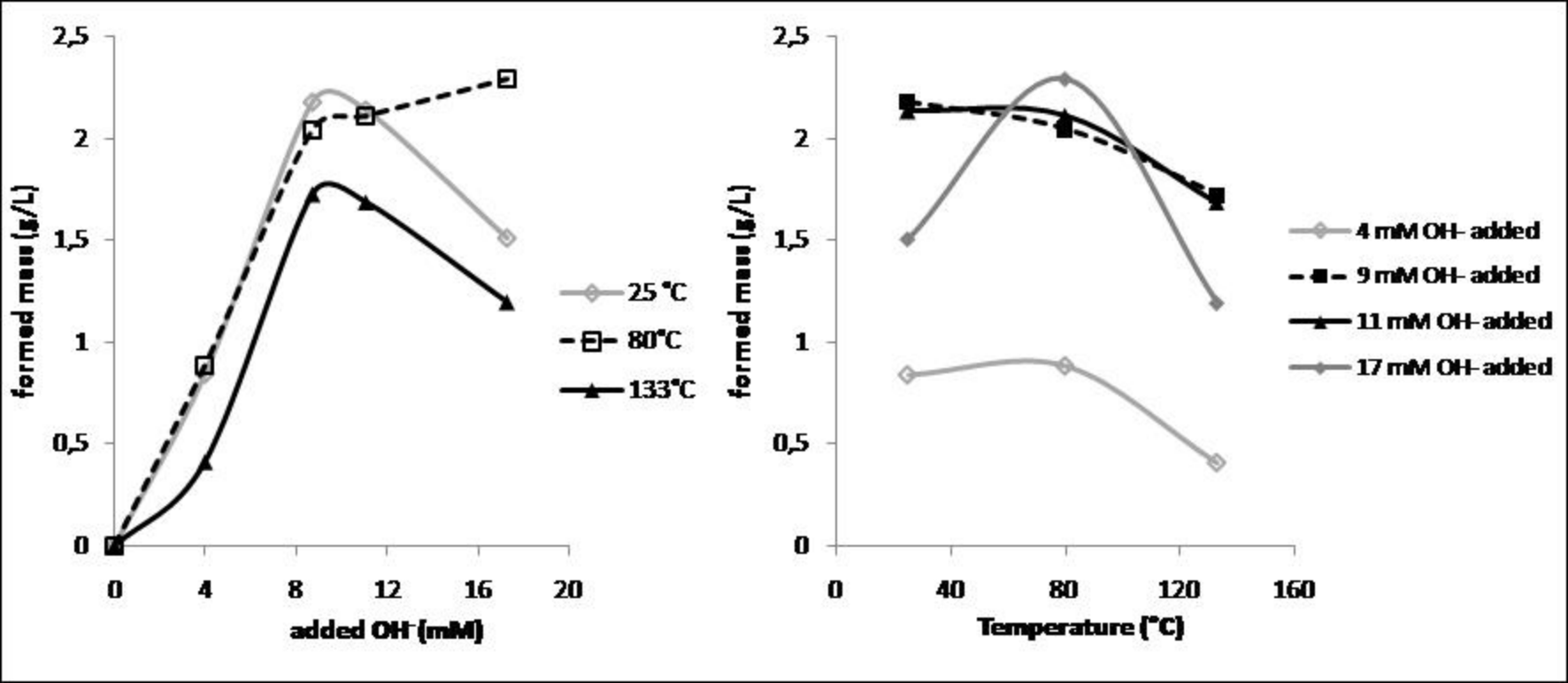
2,5
2
1,5
1
0,5
0
formed mass (g/L)
0
4
8
12
16
20
added OH- (mM)
25 °C
80°C
133°C
2,5
2
1,5
1
0,5
0
formed mass (g/L)
0
40
80
120
160
Temperature (°C)
4 mM OH- added
9 mM OH- added
11 mM OH- added
17 mM OH- added

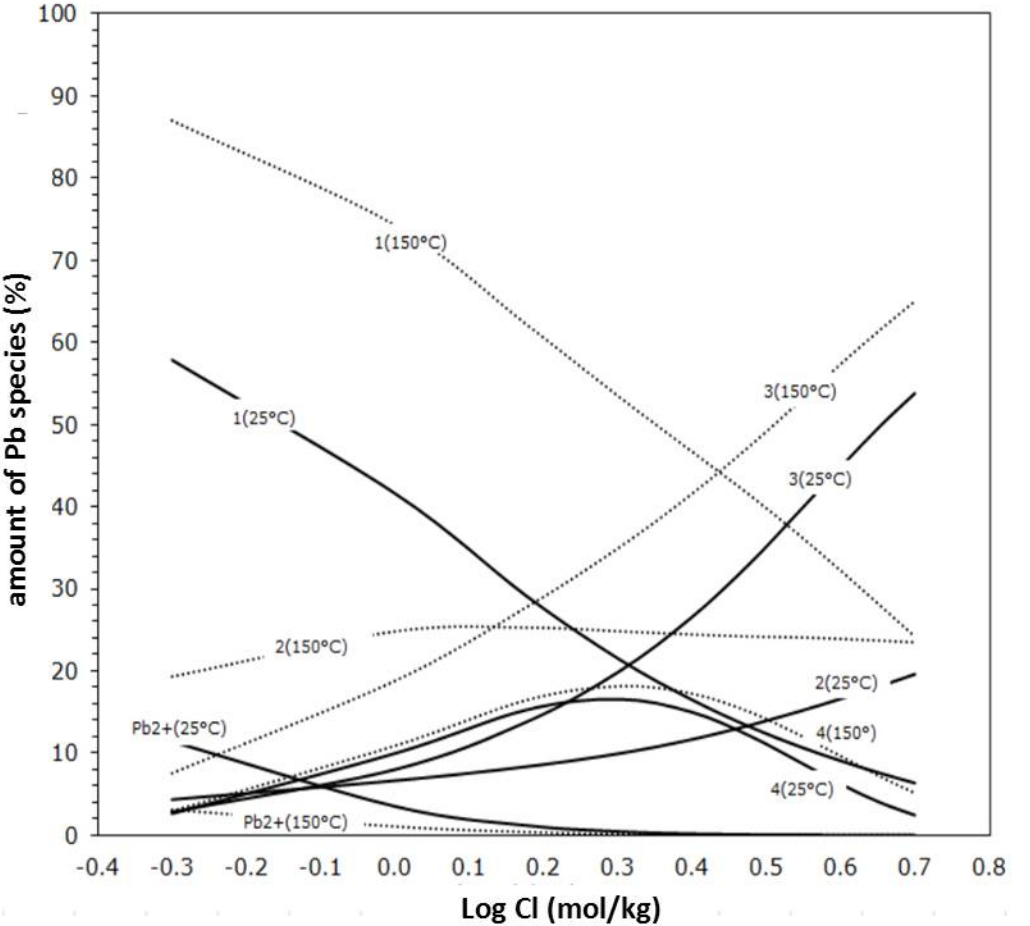
amount of Pb species (%)
Log Cl (mol/kg)
1(150°C)
1(25°C)
3(150°C)
3(25°C)
2(150°C)
2(25°C)
Pb2+(25°C)
4(150°)
4(25°C)
Pb2+(150°C)

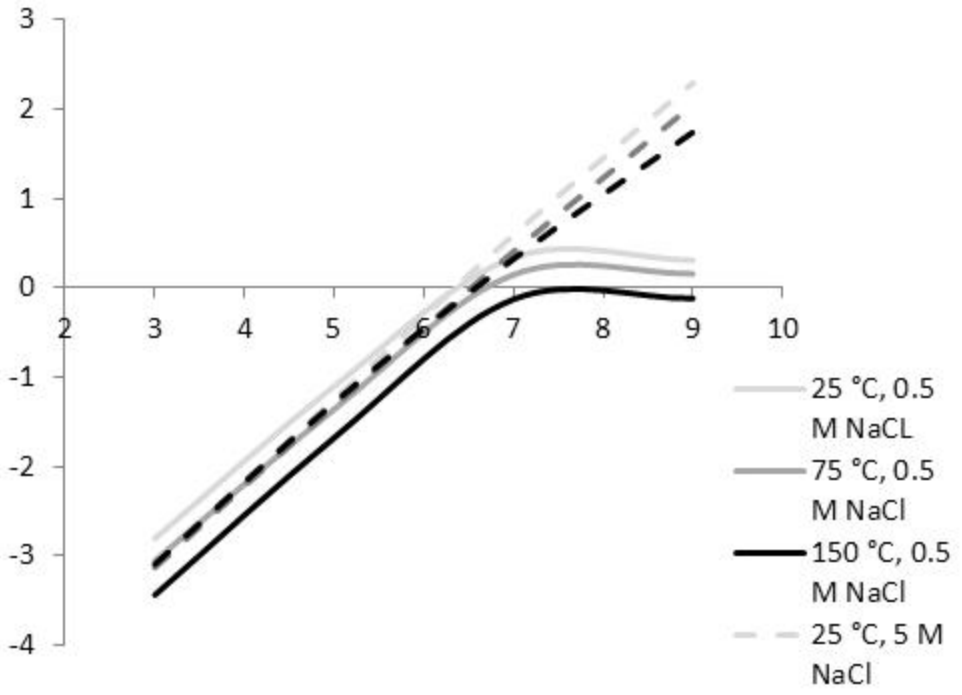
3
2
1
0
-1
-2
-3
-4
2
3
4
5
6
7
8
9
10
25 °C, 0.5 M NaCL
75 °C, 0.5 M NaCl
150 °C, 0.5 M NaCl
25 °C, 5 M NaCl

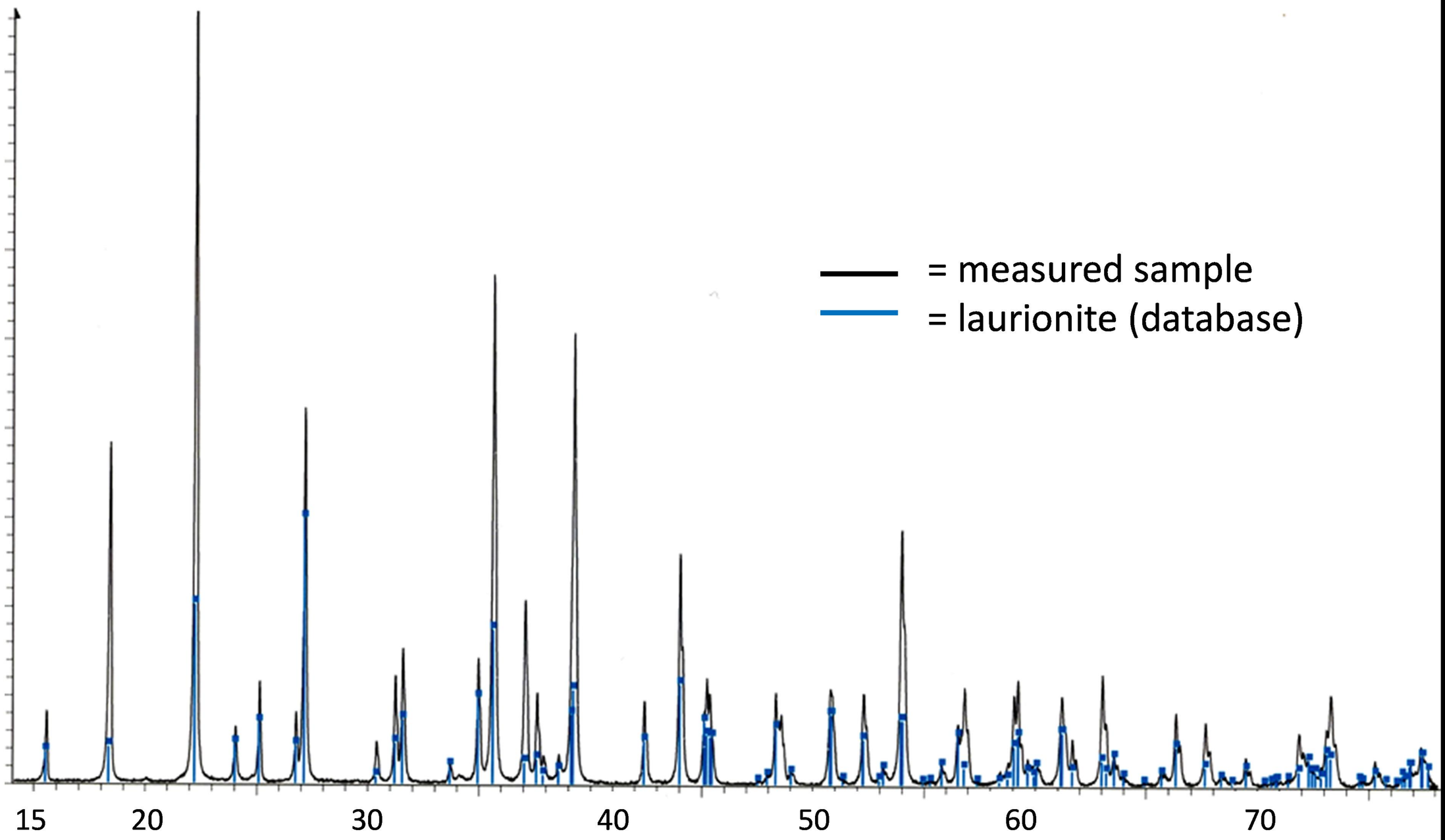
= measured sample
= laurionite (database)
15
20
30
40
50
60
70
2- Theta

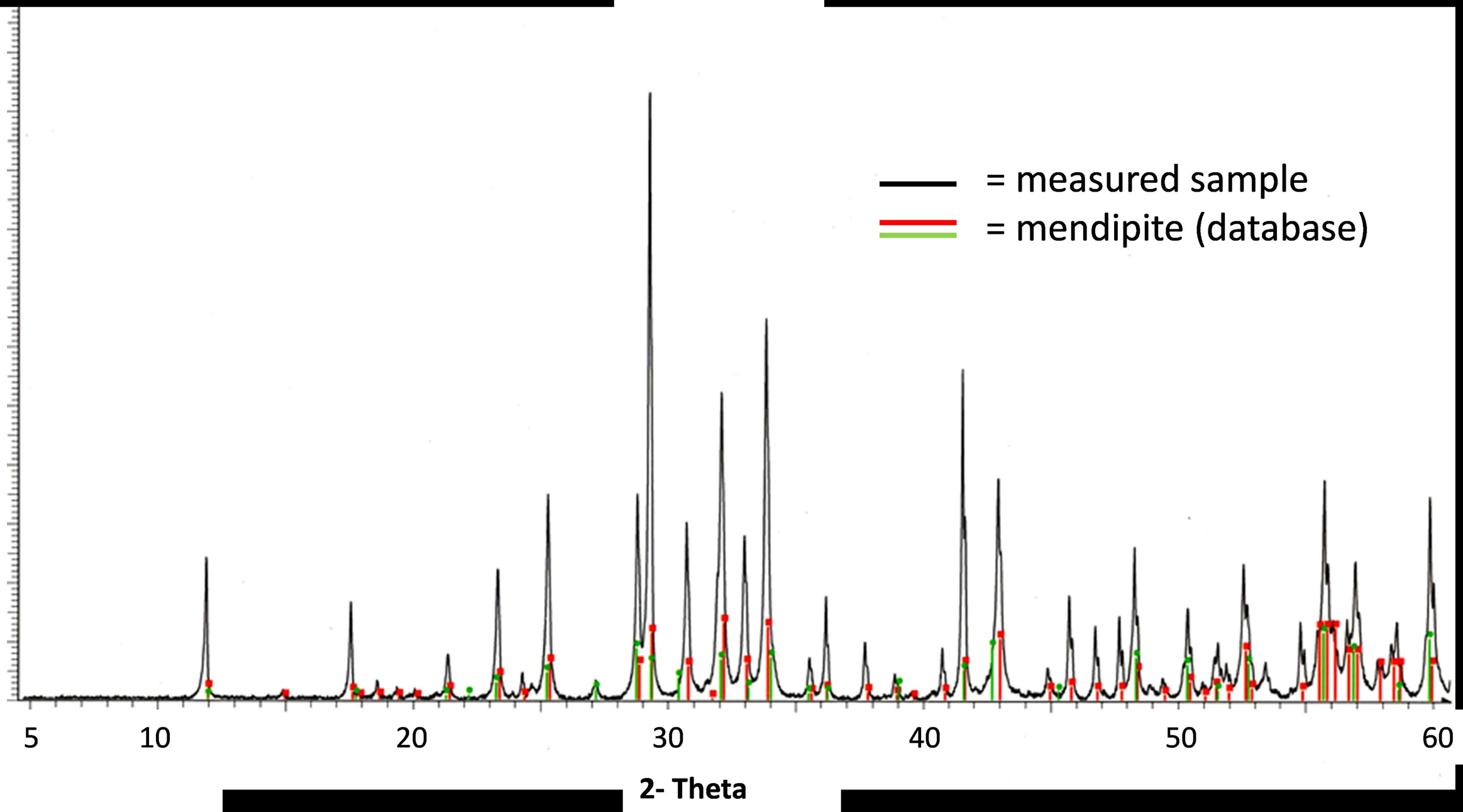
= measured sample
= mendipite (database)
5
10
20
30
40
50
60
2- Theta

25°C, 4 mM NaOH

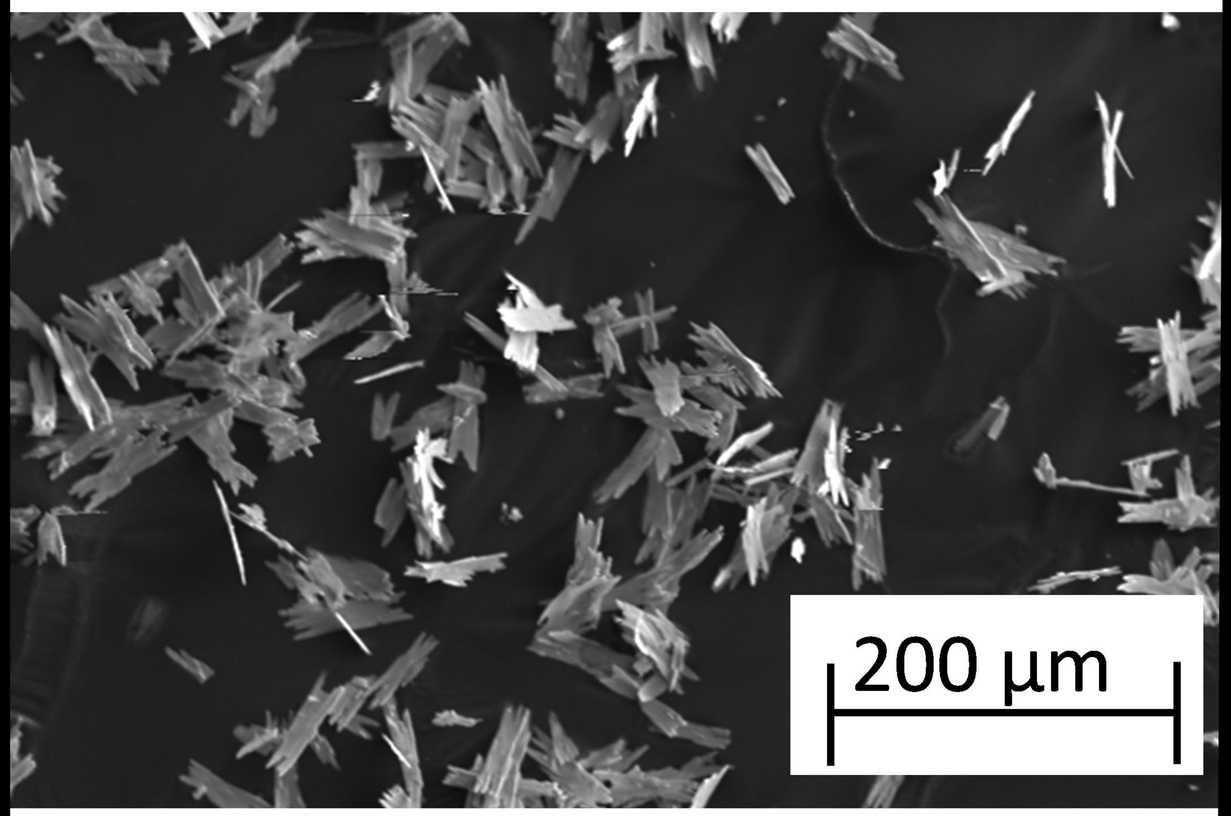

133°C, 4 mM NaOH

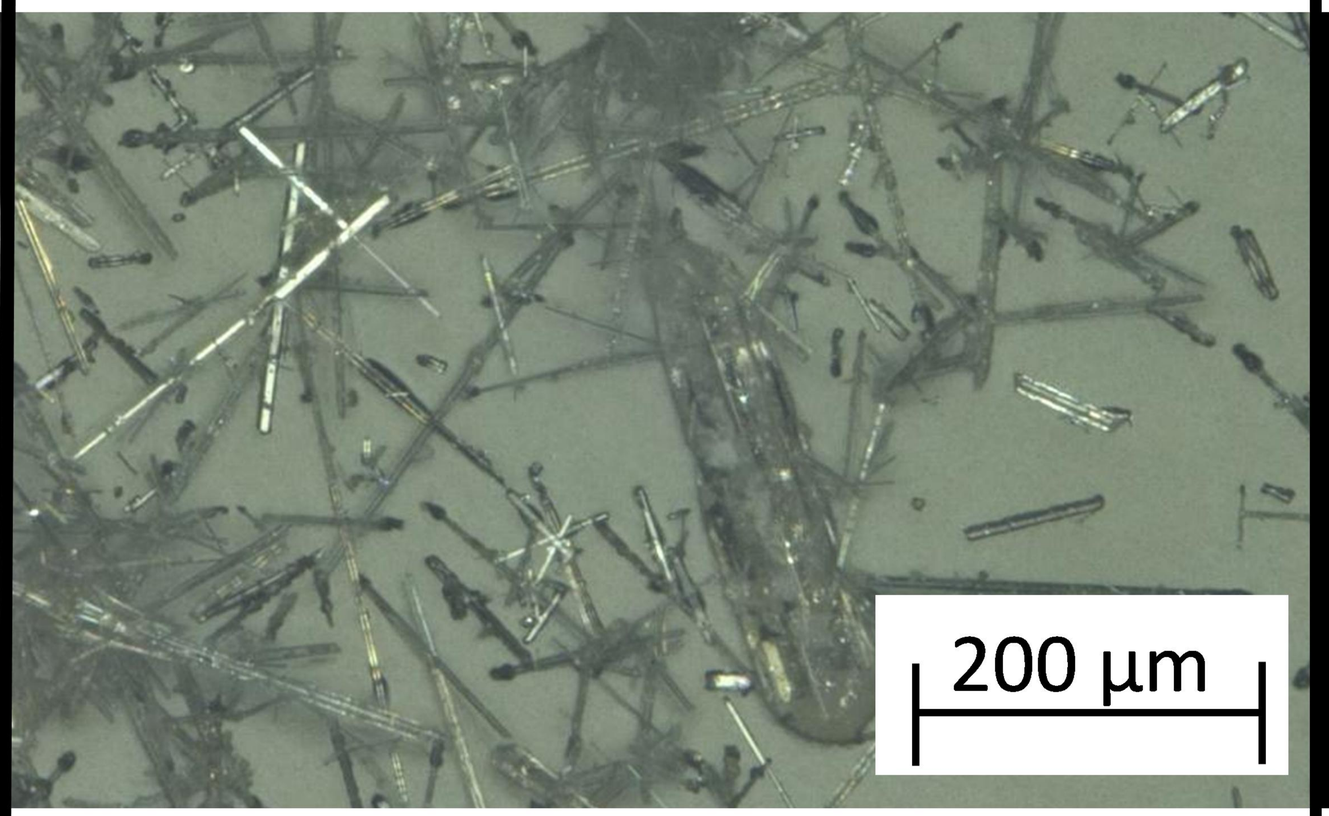

80°C, 4 mM NaOH

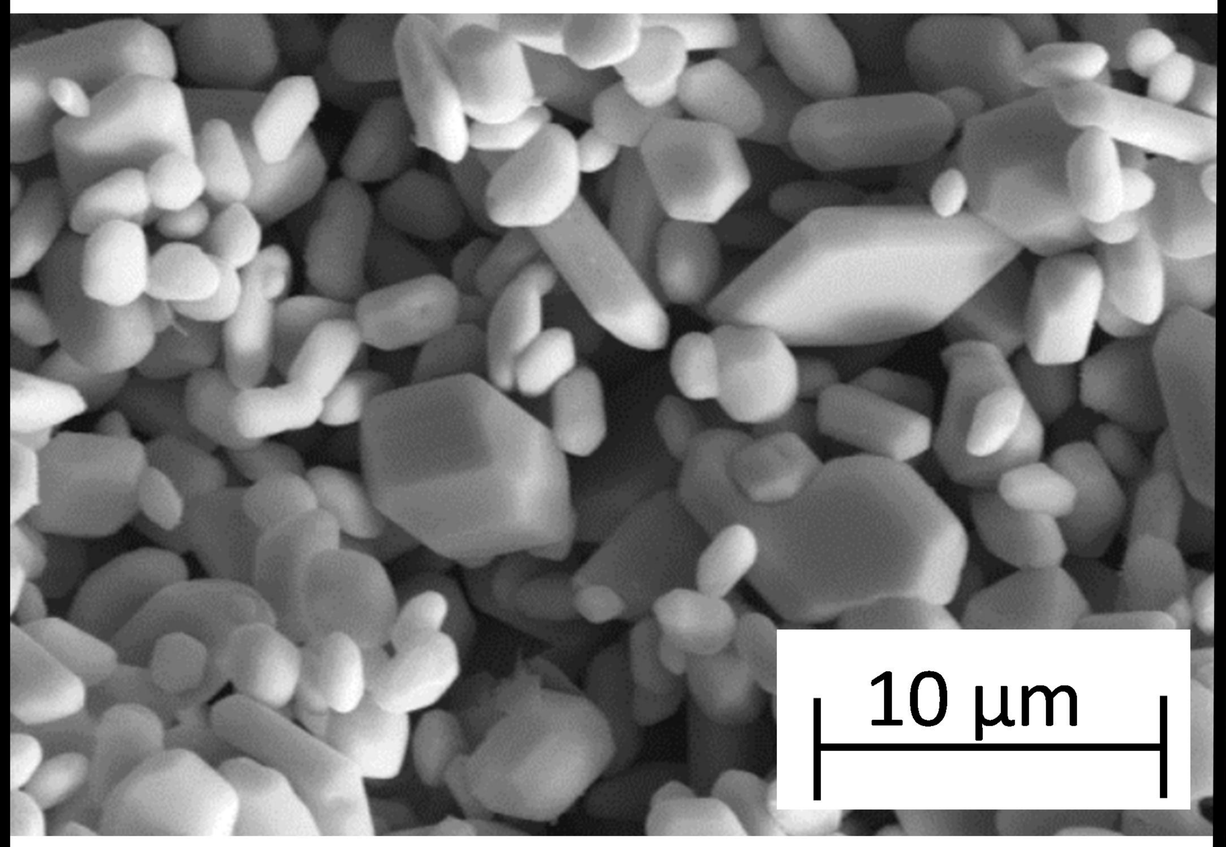

133°C, 9 mM NaOH

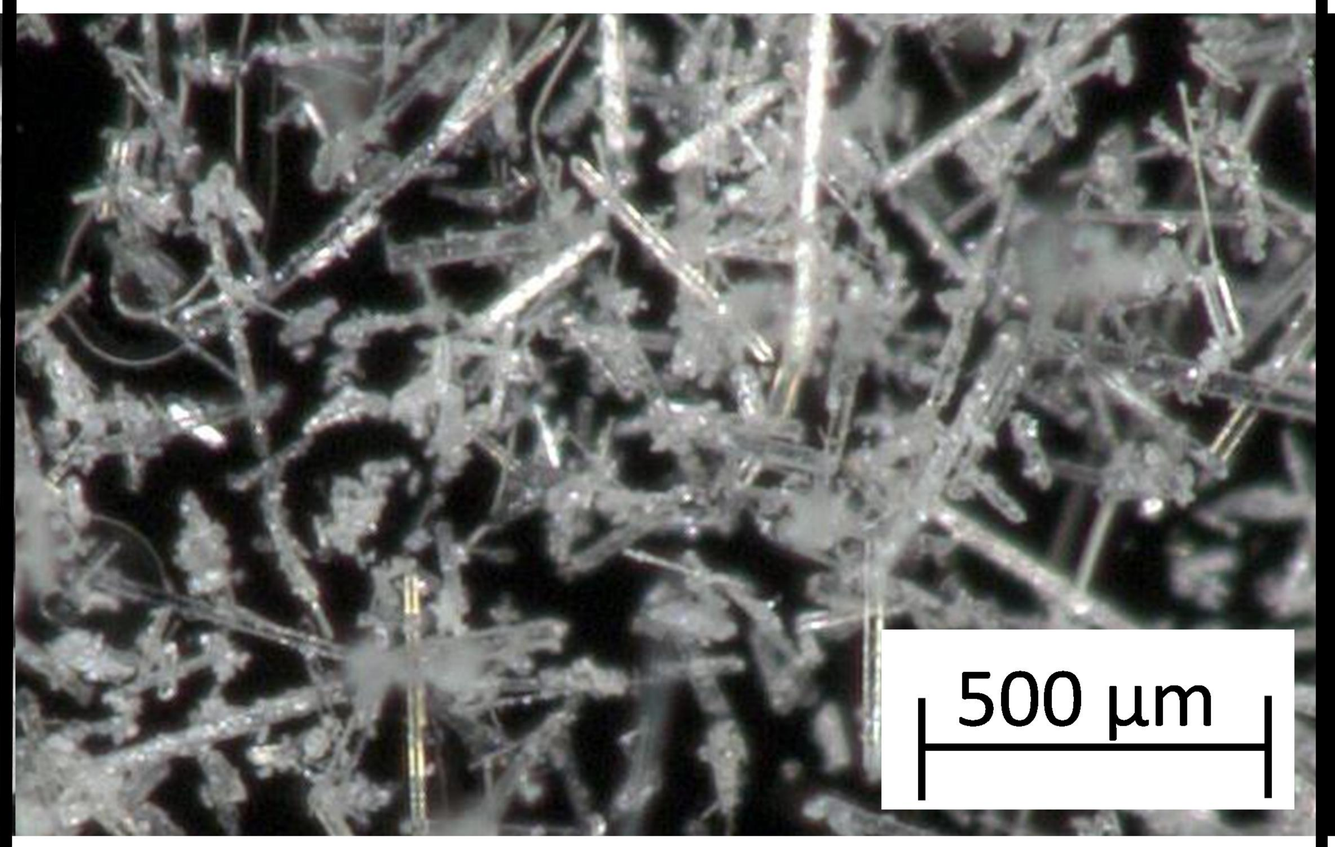

80°C, 9 mM NaOH

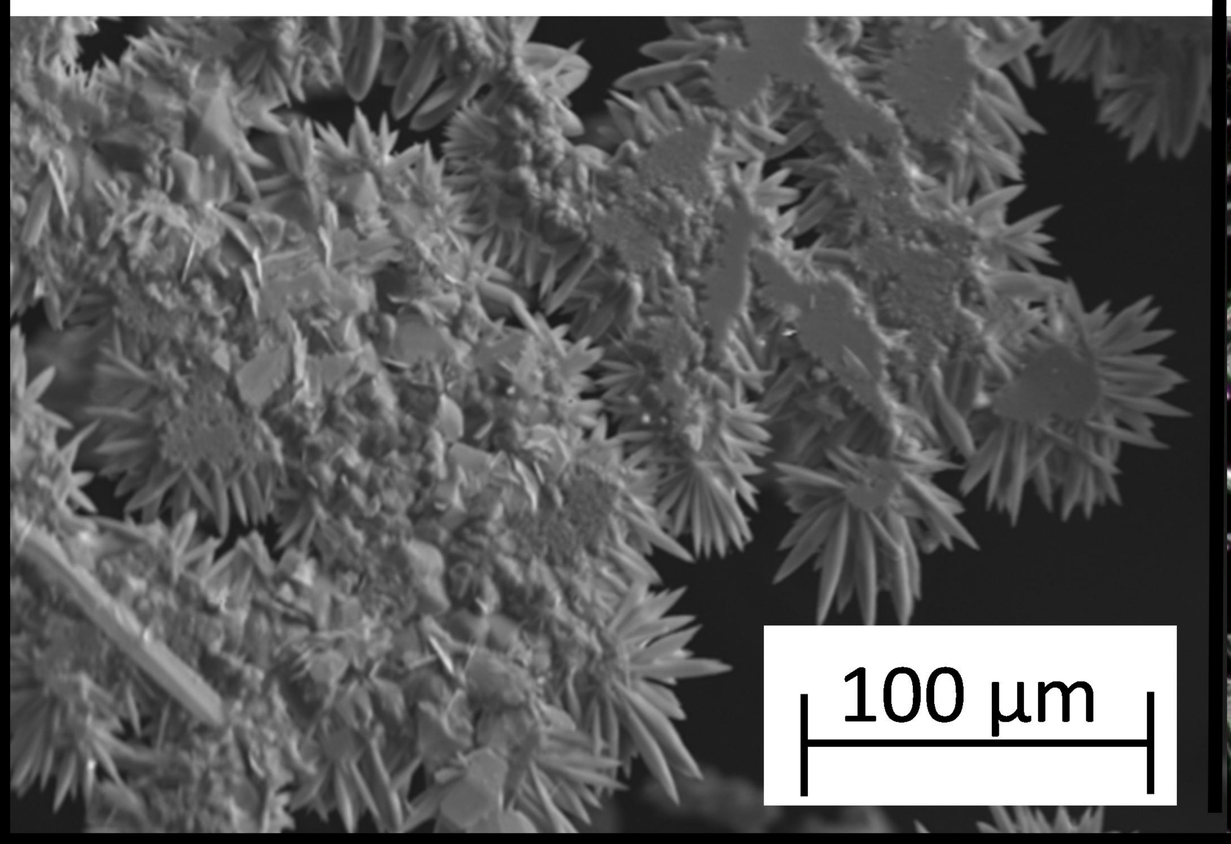

133°C, 17 mM NaOH

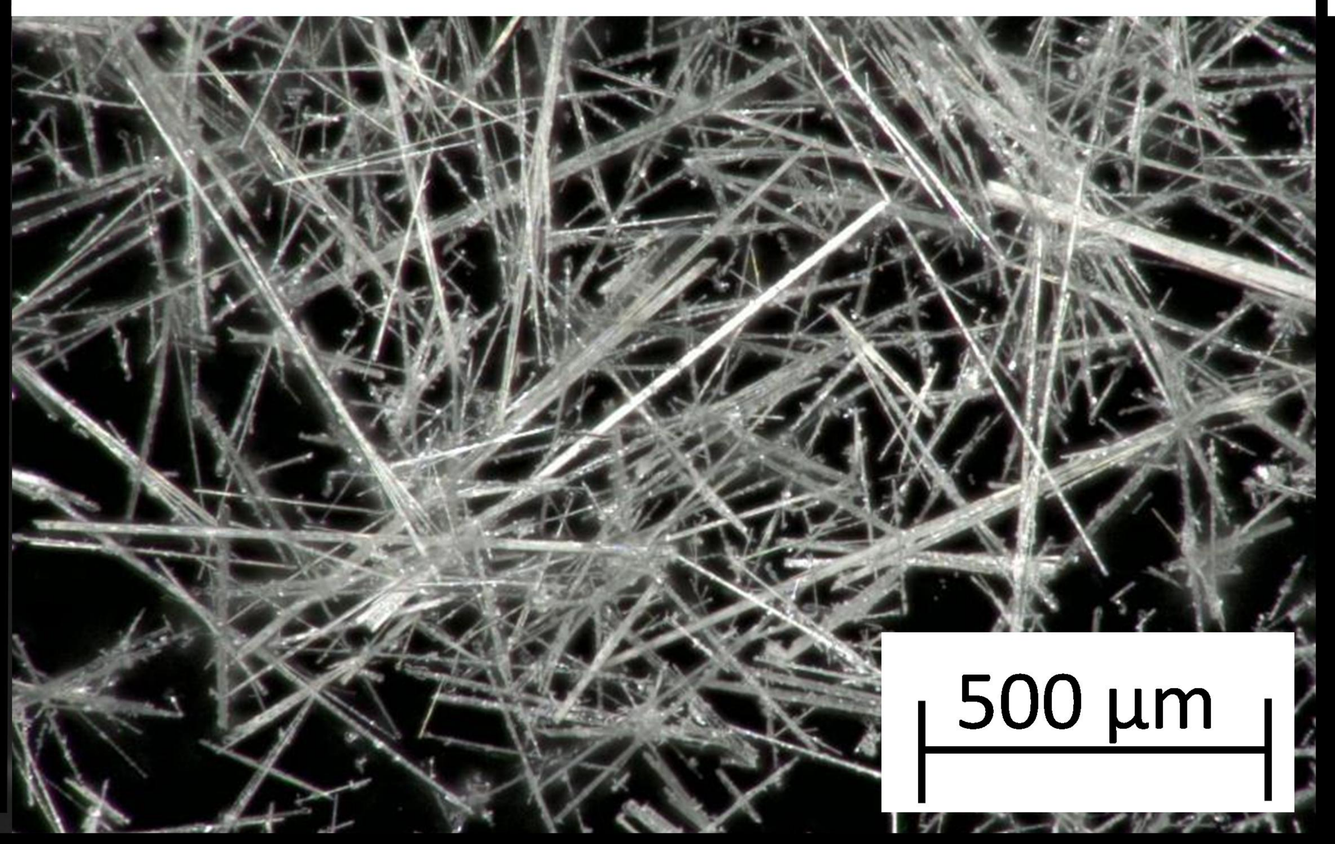

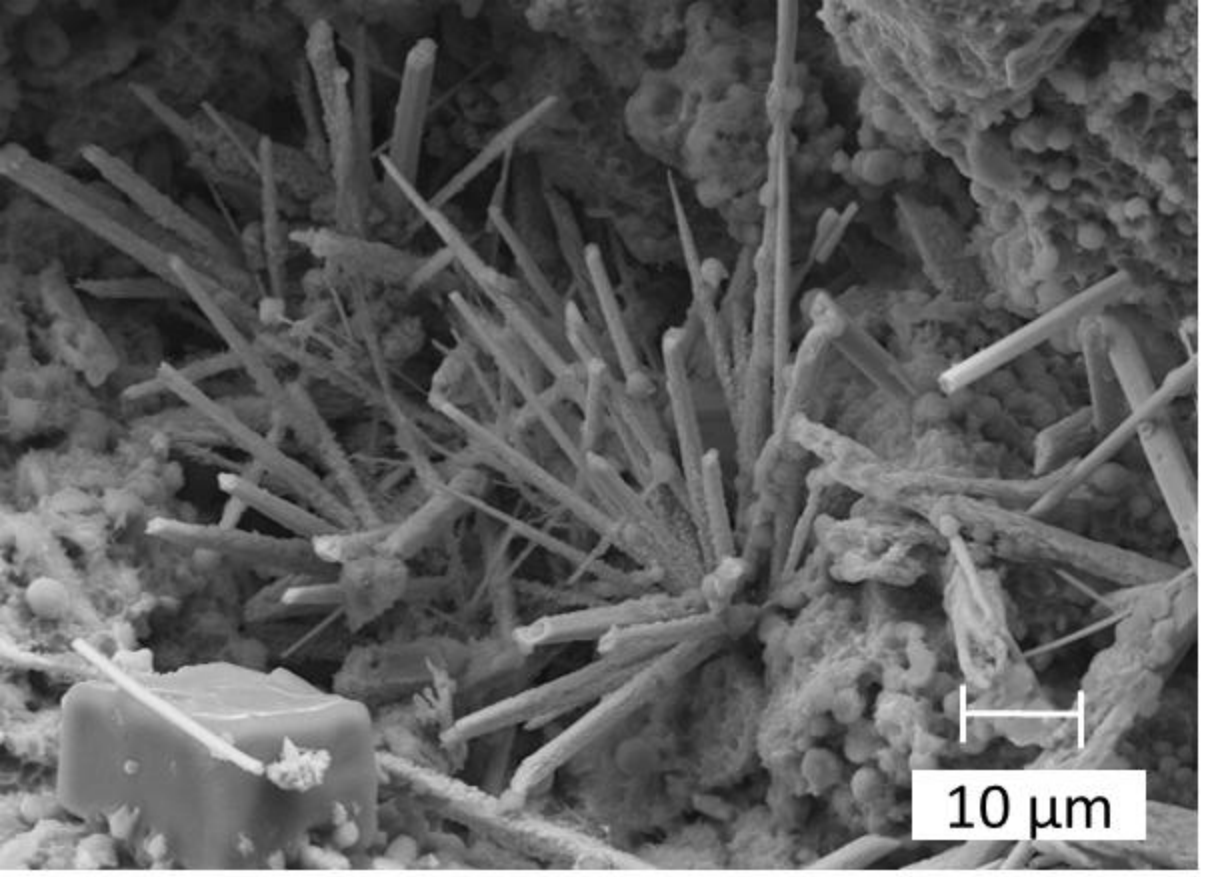
10 µm

Table 1. Aqueous and solid lead complexes with formation constants used in the speciation modeling (Geodat database, Moog and Cannapin 2014; stability constants from Luo & Millero 2007).

reaction	**log_k**
$Pb^{2+} + Cl^{-} = PbCl^{+}$	1.48
$Pb^{2+} + 2\ Cl^{-} = PbCl_2$	2.23
$Pb^{2+} + 3\ Cl^{-} = PbCl_3$	-1.82
$Pb^{2+} + 4\ Cl^{-} = PbCl_4^{2-}$	0.05
$Pb(OH)Cl + H^{+} = Pb^{2+} + H_2O + Cl^{-}$	-0.62
$H_2O + Pb^{2+} = Pb(OH)^{+} + H^{+}$	-6.25
$H_2O + Pb^{2+} = PbO + 2H^{+}$	-16.95
$H_2O + Pb^{2+} = PbO(OH)^{-} + 3H^{+}$	-27.9